Rip spacing and persistence on an embayed beach

R. A. Holman,[1] G. Symonds,[2,3] E. B. Thornton,[4] and R. Ranasinghe[5]

Received 15 March 2005; revised 7 July 2005; accepted 7 September 2005; published 17 January 2006.

[1] Four years of daily time exposure images from an embayed beach were examined to study the spacing, persistence, and location preferences of rips in a natural rip channel system. A total of 5271 rip channels was observed on 782 days. Occurrence statistics showed no evidence of the preferred location pattern associated with standing edge waves trapped in an embayed beach. The histogram of rip spacing, the primary diagnostic observable for most models, was well modeled by a lognormal distribution (mean spacing of 178 m). However, spacings were highly longshore variable (time mean of the standard deviation/longshore mean of rip spacing was 39%), so they are of questionable merit as a diagnostic variable. Storm-driven resets to the longshore uniform condition required by most models occurred only four times per year on average, making rip generation models relevant to only a small fraction of the system behavior. Rip spacings after the 15 observed reset events were uncorrelated with bar crest distance. The lifetime of the 324 individual rip channel trajectories averaged 45.6 days. Rips were equally mobile in both longshore directions, but the coefficient of variation of rip migration rates was large, even for high migration rates. The mean migration rate was well correlated to a proxy for the longshore current (R^2 of 0.78). Thus there is no significant evidence that the formation, spacing, and migration of rip channels on this beach can be explained by currently existing simple models. Moreover, the alongshore uniform initial conditions assumed by these models are rare on Palm Beach, making the models generally inapplicable.

Citation: Holman, R. A., G. Symonds, E. B. Thornton, and R. Ranasinghe (2006), Rip spacing and persistence on an embayed beach, *J. Geophys. Res.*, *111*, C01006, doi:10.1029/2005JC002965.

1. Introduction

[2] Rip currents are a common feature on surf beaches and are often a hazard to the unwary swimmer. They also provide an efficient mechanism for the cross-shore exchange of sediment, water and pollutants in the nearshore. On natural beaches, rip currents are often associated with deep, cross-shore-oriented channels from the shoreline to beyond the breakpoint, separated alongshore by shallow shoals. The succession of shoals and channels is often quite obvious and, to an observer on the beach, the rip channels appear to be quite regularly spaced alongshore. A well-defined alongshore length scale, defined by alternating shoals and channels or onshore and offshore flows, is arguably the essential characteristic of rip cell circulation behind much of the past and present theoretical treatment of rip generation.

[3] Models to explain the generation of rip currents with regular spacing can be classified as template models in which pattern scales are derived solely from attributes of the fluid forcing, or feedback models in which feedback between components of the fluid/topography system leads to the development of preferred scales [*Holman*, 1995; *Werner*, 1999; *Blondeaux*, 2001]. Of the template class, the best known are several early models, notably by *Bowen* [1969] and *Dalrymple* [1975], that produced rip current cells with regular alongshore spacing and were supported with laboratory data. In both models, alongshore variations in wave height (due to synchronous edge waves in the Bowen model and phase-locked crossing incident waves in Dalrymple's model) produce alongshore-variable wave setup and an associated rip and cell circulation system. However, these models both assume specific aspects of a forcing wave field that seem inconsistent with the stochastic forcing observed on natural beaches. *Reniers et al.* [2004] suggest that vorticity induced by wave group patterns could be sufficiently long lasting to perturb an initially alongshore uniform barred beach in a quasiperiodic way, with scales appropriate to the longshore scale of groups, itself a function of the directional spread of the incident wave field. While this serves essentially as a template for subsequent rip generation, the perturbations are less than 1 cm and require flow topography feedback to grow to significant size.

[1] College of Oceanic and Atmospheric Sciences, Oregon State University, Corvallis, Oregon, USA.
[2] School of Physical, Environmental and Mathematical Sciences, University of New South Wales, Australian Defense Force Academy, Canberra, New South Wales, Australia.
[3] Now at Floreat Marine Laboratories, Commonwealth Scientific and Industrial Research Organisation, Floreat Park, Western Australia, Australia.
[4] Oceanography Department, Naval Postgraduate School, Monterey, California, USA.
[5] Department of Infrastructure, Planning and Natural Resources, University of New South Wales, Sydney, New South Wales, Australia.

0148-0227/06/2005JC002965$09.00

[4] Alternatively, rip cells have been shown to result from flow and morphological instabilities [*Hino*, 1974; *Dalrymple and Lozano*, 1978; *Deigaard et al.*, 1999; *Falques et al.*, 1999, 2000; *Damgaard et al.*, 2002] and the alongshore length scale is associated with the fastest growing unstable mode. *Hino* [1974] predicts rip spacing approximately four times the surf zone width, consistent with the notion that the rip spacing is a function of the incident wave height, a common belief since the early observations by *Shepard et al.* [1941]. *Falques et al.* [1999, 2000] also find the preferred alongshore length scale is 2 to 3 times the surf zone width. Of the above studies, only *Deigaard et al.* [1999] and *Damgaard et al.* [2002] considered the formation of rip cells on an initially barred beach, finding a preferred ratio of rip spacing to offshore bar distance of 1.8 and between 1.4 and 5.7, respectively. *Murray and Reydellet* [2001] introduce an instability mechanism that relies on feedback between wave propagation and an incipient rip, showing the expected growth of rips with spacings appropriate to nature.

[5] While rip spacing remains one of the fundamental diagnostic features used to assess the validity of a variety of rip generation models, few long-term, systematic observations of rip spacing on a natural beach have been reported. Nineteen months of daily visual observations of rip locations at Narrabeen Beach, Australia, were reported by *Short* [1985] and later reexamined by *Huntley and Short* [1992]. Both of these analyses produced surprisingly poor correlations between rip spacing and wave height, surf zone width and wave period. *Huntley and Short* [1992] note the poor correlations may be due in part to the uncertainties in the visual observations, particularly estimates of surf zone width.

[6] More recently, long-term monitoring of nearshore morphology with high spatial and temporal resolution has become possible with the application of video imaging techniques [*Lippmann and Holman*, 1989]. Rip channels are quite clearly visible in time exposure video images because of reduced wave breaking in the channels relative to the adjacent shoals. *Ranasinghe et al.* [1999] use 2 years of daily time exposure images to characterize rip channel statistics on the northern end of Palm Beach, Australia. *Ruessink et al.* [2000] used combined survey and time exposure video data to characterize a 6-week record of sandbar variability on the Dutch coast, explaining the dominant variability with longshore migration of the bar pattern at rates of up to 150 m/day. *van Enckevort et al.* [2004] compared video observations of crescentic bar systems at four distinct field sites, noting large intersite and temporal variations in bar spacing. They also observed considerable longshore variability of crescentic bar wavelengths, in contrast to the periodicity predicted by several generation hypotheses, for example generation by standing edge waves [*Bowen and Inman*, 1971]. While these latter two papers do not directly address rip currents, crescentic bars and longshore variations in sandbar topography are often linked to rip currents.

[7] The purpose of this paper is to characterize the statistics of a natural rip system based on 4 years of daily observations of an embayed beach located in a microtidal, swell-dominated coastal environment. Observations are based on time exposure images, as above, and the analyses will address statistics of the rip current system that are diagnostic in testing the generation mechanisms discussed above.

2. Study Site

[8] Palm Beach, located about 30 km north of central Sydney, Australia, is a 2 km-long embayed beach located in a microtidal, swell-dominated coastal environment (Figure 1). The nearshore bed slope at Palm Beach is 0.02 [*Brander*, 1999] while the median grain size in the surf zone is 0.30 mm [*Wright et al.*, 1980]. The mean significant deep water wave height is about 1.5 m, increasing to 3–6 m during cyclonic events, while the dominant wave direction is from SSE with occasional E and NE swells [*Short and Trenaman*, 1992]. There is no significant seasonal variation in the offshore wave climate [*Short and Trenaman*, 1992].

[9] The nearshore morphology at Palm Beach exhibits all four intermediate beach states described by *Wright and Short* [1984]. The morphological evolution of a single rip cell on Palm Beach was described by *Brander* [1999] as follows. Following a period of high waves, referred to here as a reset event, the beach typically exhibits a shore-parallel bar approximately 100 m offshore. *Wright and Short* [1984] refer to this state as Longshore Bar Trough (LBT). During the subsequent period of lower waves, the bar slowly migrates onshore [*Symonds et al.*, 1997] while developing longshore variability and rip channels. Under suitable conditions, the morphology can progress through the Rhythmic Bar Beach (RBB), Transverse Bar Rip (TBR), to Low Tide Terrace (LTT) beach state, all of which are described by *Wright and Short* [1984]. However, this sequential progression can be interrupted at any stage by another high-wave event, in which case the morphology would return to the LBT state and the cycle repeats. These observations were reconfirmed and refined through analysis of 4 years of daily time exposure images obtained at the same beach and the morphodynamics processes of the state transitions investigated through numerical modeling by *Ranasinghe et al.* [2004].

3. Data

3.1. Video Images

[10] In January 1996, an Argus video-imaging station [*Holman et al.*, 1993; *Aarninkhof and Holman*, 1999; *Holman et al.*, 2003] was installed in Barranjoey lighthouse, 115 m above mean sea level (Figure 1). While the station included two south facing cameras, analyses for this paper will be based on only one, C1, a wide-angle view that spanned 90% of the beach (Figure 2). The basic data of interest are 10-min time exposure images, collected each daylight hour (Figure 2). Hourly images from each day were themselves averaged to create a "daytimex," a composite image that combined information throughout the range of the tide.

[11] At station installation, the location of the camera and of a number of clearly visible ground control points (GCPs) were surveyed relative to a known benchmark. From comparison of the image and world location of the GCPs, the photogrammetric transformation from image to world space was computed using the technique presented by

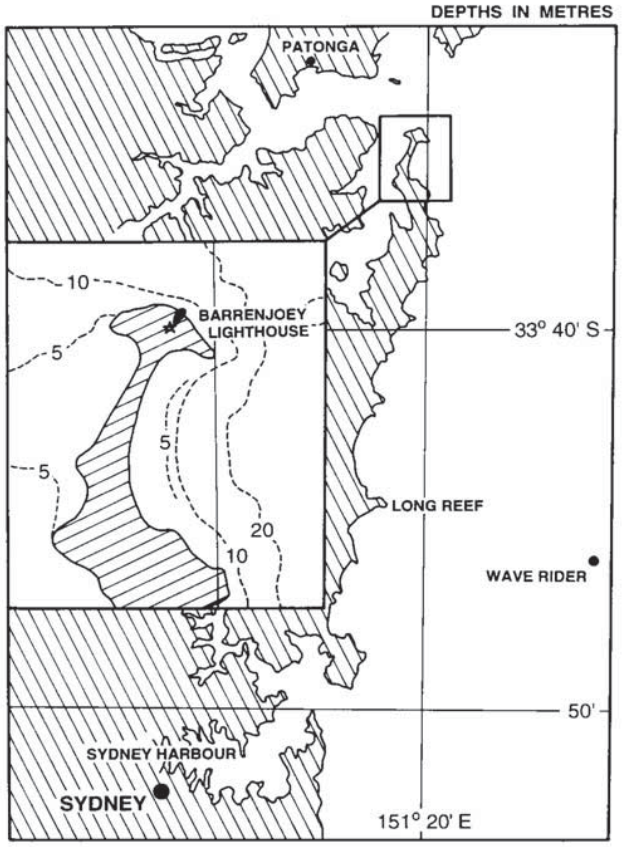

Figure 1. Location map of Palm Beach, Australia. The video cameras are installed in Barranjoey lighthouse, 115 m above sea level. Deep water wave statistics are available from the wave rider off Long Reef, and tides are measured at the coastal port of Patonga.

Holland et al. [1997]. Accuracy of this process is typically one pixel. At midbeach, one pixel corresponds to a ground accuracy of 0.9 and 7.3 m in the cross-shore and alongshore directions, respectively, worsening to 4.1 and 23.0 m at the far end of the beach.

[12] Time exposure images were transformed into rectifications (map views) through mathematical projection onto a horizontal plane located at mean sea level (Figure 2b [*Holland et al.*, 1997]) to allow georeferenced digitization of rip channel locations. However, the shoreline at Palm Beach is curved, complicating the definition of alongshore distance in the following analyses. To compensate, a new definition of alongshore was established by fitting a set of midsurf zone Argus locations to a log spiral function [*Komar*, 1998]

$$r = r_0 e^{(\cot \mu)\alpha}, \tag{1}$$

where r is measured radially from an origin at $\chi_0 = 525$, $\psi_0 = -500$, relative to the Argus image coordinates (χ positive offshore from the mean shoreline and ψ positive in the mean alongshore direction in a right-hand coordinate sense with z positive up) and the angle α ranged from 0 to π. The best fit parameter values were $r_0 = 1.65$ and $\cot \mu = 2.404$ (Figure 2b). Rip channel locations along this curve were transformed from χ, ψ Argus coordinates to an alongbeach location, y, by computing the length of the curve from $\alpha = 0$ to the rip position as the integral of the norm of the derivatives of the equations for the χ and ψ coordinates of the log spiral.

[13] The locations of bright bands of wave breaking in time exposure images have previously been shown to correspond well to the locations of submerged sandbars [*Lippmann and Holman*, 1989; *van Enckevort and Ruessink*, 2001]. Similarly, gaps in breaking patterns correspond to topographic rip channels that incise a surrounding sandbar [*Ranasinghe et al.*, 1999, 2004]. An example of TBR morphology can be seen in the time exposure image of Palm Beach shown in Figure 2. Rip channels are clearly visible as low pixel intensity (dark) regions extending across the surf zone, bounded by high pixel intensity (bright) regions over the shoals between the rip channels.

3.2. Rip Locations

[14] *Ranasinghe et al.* [1999] identified rip channels as local minima in alongshore profiles of pixel intensity transects, taken approximately at midsurf zone. While adequate for simple cases, this automated approach was found to be sensitive to parameter choices in the analysis and often gave results in disagreement with visual assessment. After considerable experimentation it became clear that no simple algorithm provided robust location of rip locations under the range of conditions exhibited at this site. Thus it was decided to base this work on a process of manual identification of rip channel locations, $y_r(n, t)$, where n is an index for each of the set of the 1 to $N_y(t)$ rip locations for each day and t is time. The rip locations in y_r are ordered by increasing value.

[15] The manual selection was done by author G. Symonds (GS) on one daytimex image per day for the period 1996–1999 inclusive. To determine confidence limits on both the occurrence and locations of sampled rip currents, replicate sampling was carried by author R. Ranasinghe (RR) for the data from 1996. Figure 3 shows a subsection of the 305-day comparison data set. Agreement is good, although some differences occur in both the duration over which rips were deemed to exist and their exact longshore locations. Comparison revealed that both users digitized an average of 7.2 locations per day in common, while differing on an average of 1.1 rip locations (Table 1). For the agreed-upon rips, the RMS difference in alongshore location averaged 13.2 m (a bias of 5.1 m and standard deviation of 11.8 m; see Table 1). As a further test, two nonspecialists digitized the same data set after only basic instruction. Comparison statistics between these data and the data set under study (done by GS) reveal similar, if slightly worse, RMS error statistics (Table 1). Overall, it is believed that the RMS error of individual rip current locations is about 12 m. Interestingly, comparisons for rips in the near field ($y_r > 1000$) were only about 20% better than those farther away ($y_r < 1000$), indicating that pixel resolution was not a significant problem.

[16] From Figure 3 it is clear that, rather than considering rip current locations as independent daily events, they should be considered as coherent structures with trajectories of alongshore location versus time, $\mathbf{y_i}(t)$, whose statistics

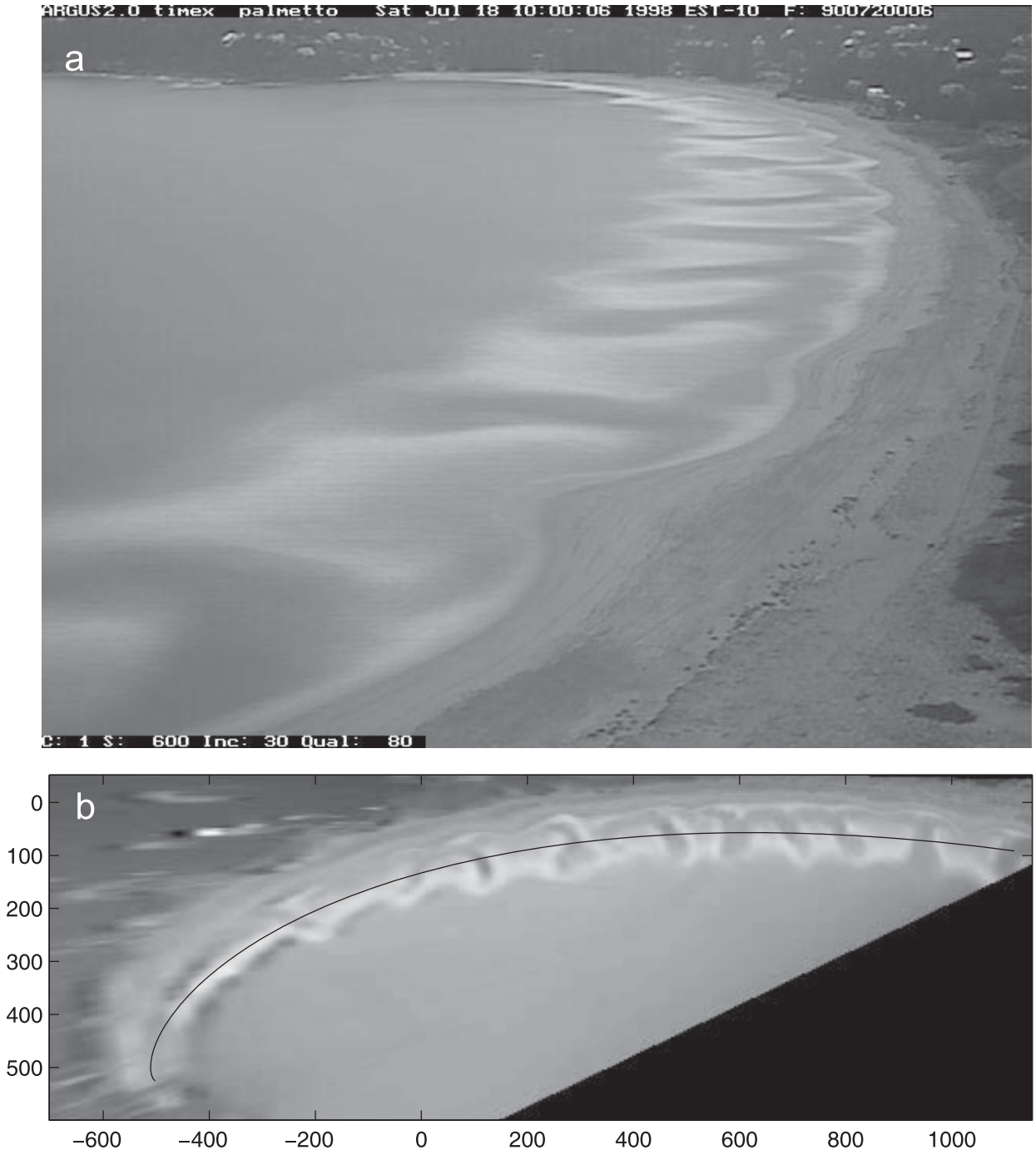

Figure 2. (a) Oblique time exposure image of Palm Beach from 18 July 1998 and (b) rectification of the same image. Rip channels are indicated by dark cuts through the white nearshore dissipation patterns. Axes in Figure 2b indicate cross-shore and longshore coordinates in meters, defined in a local Argus coordinate system, χ and ψ. The curved line indicates the best fit of a log spiral shoreline curve to the midsurf zone region. The longshore coordinate for the analyses in this paper, y, was defined by integrating along this curve.

can be analyzed (the symbol $\mathbf{y_i}$ is in bold font to help distinguish rip trajectories from daily rip location vectors). The linking of individual daily rip locations into trajectories was based on a nearest neighbor analysis between rip locations from adjacent days, with an additional criterion that no change in alongshore location could be greater than 75 m. Gaps exist in the data set because of fog, instrument failure or low waves (hence no breaking signatures for rip location). To account for these gaps, automated matching was attempted as far back as 4 days.

[17] When the resulting set of rip trajectories, $\mathbf{y_i}(t)$, were graphed, it was apparent that some manual intervention was still necessary. For example, often rip trajectories were clearly continuous across low-wave data gaps longer than

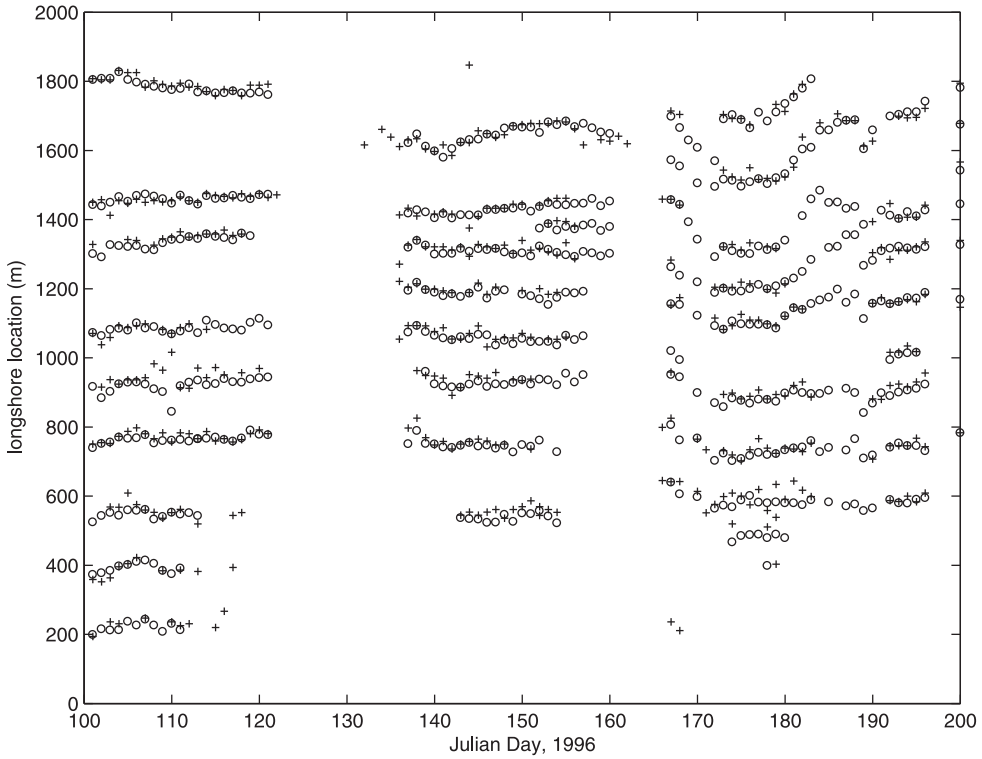

Figure 3. Subsection of the replication test results comparing the locations of rips for 1996 as digitized by G. Symonds (pluses) and R. Ranasinghe (circles). While agreement is good, some differences exist between the durations over which individual rips were deemed to have occurred as well as their exact longshore locations. Statistical comparison was based on Julian days 61–365, 1996.

4 days and needed to be linked. In other cases of extreme rip mobility, automated linking across short data gaps appeared to jump between adjacent rips (for example, after a 3-day gap during a period of steady alongshore migration of rips, an adjacent rip may have become the closest to the original position). Fine tuning of trajectory data was done by careful visual examination of movie loops of the original imagery, played back and forth until the appropriate set of linkages was clear. This process resulted in the addition of a number of linkages and corrections of others. In all cases, rip trajectories were not connected unless there was clear evidence to do so. Questionable links were left disconnected. The resulting set of rip trajectories for the 4 years of data are shown in Figure 4.

[18] Since the majority of the theories of rip current generation assume an initial, alongshore uniform beach condition, the times of such "system resets," τ_j, were determined. A reset was defined as a high-wave event after which the preexisting rip channel topography was deemed to have no influence on the morphology following the storm (see Figure 5, for example). Four investigators examined animations of the time exposure image sequences and picked out times of resets. An objective threshold criterion for these resets was searched for, on the basis of combinations of simple external forcing parameters. The best combination was found (by empirical comparison to visual assessment) to be $H_{rms}^2/\cos\theta > 2.2$, where H_{rms} and θ are the RMS wave height and direction, described further below. However, it was found that initial conditions such as offshore distance to the sandbar and magnitudes of alongshore bathymetric variability at the time of a potential reset storm introduced substantial variation, and no single criterion was adequate to objectively identify all reset events. The final reset times were determined as any event chosen by at least three of the five criteria (four manual assessments plus the wave parameter criterion; Table 2). The 15 selected reset events are shown as vertical lines on Figure 4.

3.3. Sandbar Location

[19] The extraction of bar position from video images has been the subject of a number of studies [*Lippmann*

Table 1. Comparison of Rip Location Statistics Among Four Investigators[a]

Digitizer	$\langle\langle dy_i\rangle_y\rangle_t$, m	$\langle\langle std(dy_i)\rangle_y\rangle_t$, m	$\langle rms(dy_i)_y\rangle_t$, m	$\langle N_{\mathrm{match}}\rangle_t$	$\langle N_{\mathrm{miss}}\rangle_t$
GS-RR	5.1	11.8	13.2	7.2	1.1
GS-alt 1	−1.5	13.2	14.1	5.9	1.9
GS-alt 2	−1.3	12.8	13.4	7.2	2.5

[a]GS is G. Symonds and RR is R. Ranasinghe, who have experience in the problem, while alternates 1 and 2 were given only basic instruction. For each comparison, the number of matching locations, N_{match}, were determined for each day as well as the number that did not match, N_{miss}. The location difference, dy_i, was found for each match for each day and mean, standard deviation, and RMS statistics computed. These were averaged over the data set. Subscripts indicate dimension of statistic (time or y), while angle brackets indicates mean over the indicated dimension.

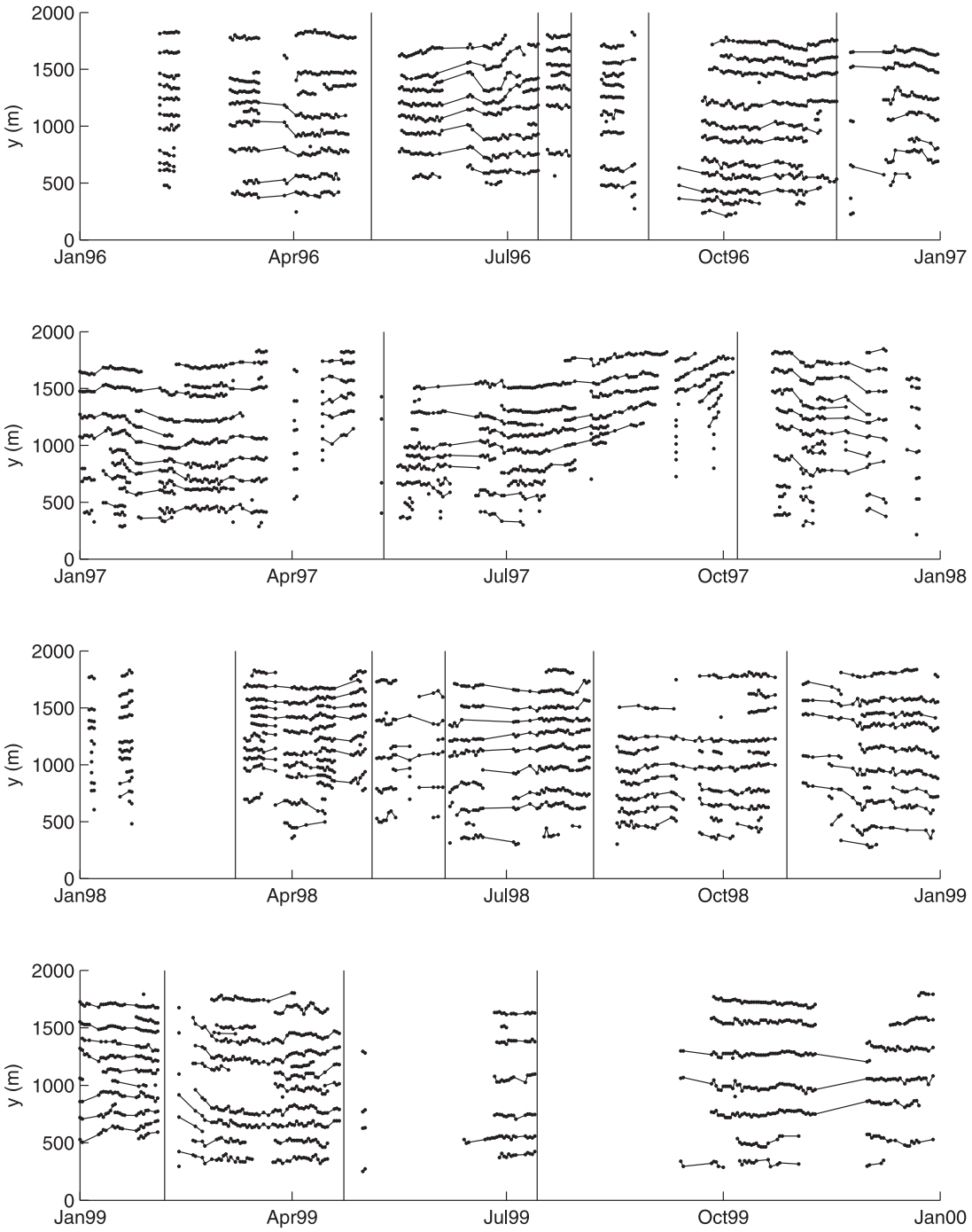

Figure 4. Rip trajectories from 1996 to 1999. Lines join each trajectory, with markers at each digitized location. Vertical bars mark system resets due to storms.

and Holman, 1989; *van Enckevort and Ruessink*, 2001; *Alexander and Holman*, 2004], all based on the assumption that peaks in cross-shore optical intensity profiles due to wave breaking reflect the position of the underlying sandbars. As part of a multisite morphodynamics study, *Alexander and Holman* [2004] extracted daily bar positions on Palm Beach for 1996–2000. To reduce noise in bar crest position estimates, cross-shore intensity profiles were fit with a Gaussian form and the bar crest position assumed to be the center value from the best fit Gaussian. To reduce noise due to tidal variations, estimates were made at high and low tide, then linearly transformed to mean sea level to yield one estimate per day. This method was used to determine the bar position at 10m intervals along the beach then averaged to obtain the mean bar position.

3.4. Waves and Tides

[20] In analyzing the rip location data, sea surface elevation and incident wave statistics are also required. Tidal

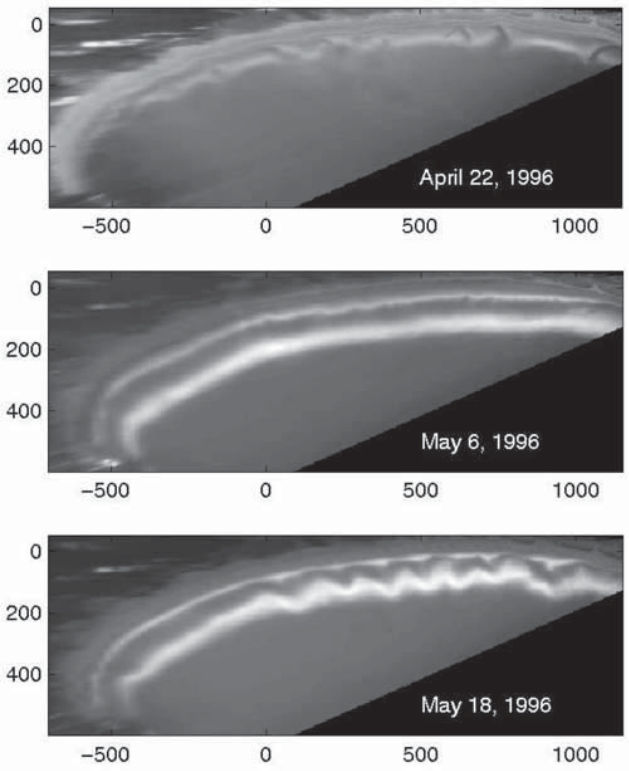

Figure 5. Sequence of rectified images showing a system reset just before 6 May 1996. Evidence of previous channels is erased, and the subsequent rip channel formation (16 May) bears no relation to the prior pattern.

elevations were obtained at 15-min intervals from a tide gauge at Patonga (Figure 1), while hourly deep water wave statistics were obtained from a directional wave rider at Long Reef (Figure 1) in a depth of 80 m. Corresponding time series of the nearshore incident wave field were required to examine the relationship between rip spacing and the incident wave forcing. Since the dominant deep water wave direction is from the SSE, the waves must undergo considerable refraction before reaching Palm Beach, which faces approximately east. The hourly, deep water wave height and direction were smoothed vectorally using a 25-point running mean then decimated at daily intervals. Inshore (10 m depth) daily root-mean-square (RMS) values of wave height, H_{rms} were estimated over the 4-year study period using the HISWA wave refraction model described by *Holthuijsen et al.* [1989]. The model parameters were tuned by comparing predicted root mean square wave heights with observations of nearshore wave heights measured in October 1999. A comparison of the same data with HISWA predictions has been reported by *Reniers et al.* [2001]. A time series plot of the resulting H_{rms} is shown in Figure 6.

4. Results

4.1. Alongshore Distribution of Rip Locations

[21] Palm Beach is characterized by the common occurrence of a suite of many rip channels with quasi-regular spacing (Figure 4). A histogram of the rip count, N, from all days of sampling for which at least one rip current was observed is shown in Figure 7. Since the mean number of rips, 6.7, is not small and the distribution has a near-Gaussian shape with a standard deviation of 2.3, it is expected that the present data set should provide a good statistical description of rip current spacing.

[22] To test for the existence of preferred rip locations associated with standing edge wave trapped between headlands, histograms were created of the probability of rip occurrence as a function of alongshore location, on the basis of 50 m bins, for each of the 4 individual years. From these 4 years, the temporal mean and standard deviations were found for each alongshore bin (Figure 8). Confidence intervals are based on the alongshore average of the standard deviation values, computed for alongshore locations between 600 and 1600 m (to avoid bias due to partial wave shadowing at the far southerly end of the beach and the obscured field of view at the near end). There is no evidence for preferred locations for rip currents, such as would be expected from models of longshore standing wave motions, trapped within the pocket beach [e.g., *Bowen and Inman*, 1971].

4.2. Rip Channel Spacing

[23] Alongshore rip spacing statistics, $d_i(t)$, were determined as the differences in alongshore location between adjacent rips for any day for which rip currents existed,

$$d_i(t_j) = (y_r(i+1, t_j) - y_r(i, t_j). \quad (2)$$

Figure 9 shows the probability distribution of rip spacing, d, based on 25 m bins, for all rip pair occurrences over the 4 years of sampling. The mean, mode and standard deviation of the rip spacing data are 178, 125, and 90 m, respectively. Less than 1% of the data showed rip spacing of less than 62.5 m (the edge of the 75 m bin). The distribution seems well modeled by a lognormal distribution, with the best fit curve shown as a solid line in Figure 9.

[24] There was concern that alongshore trends may have been present in the rip spacing data, perhaps associated with variations in the direction of shore normal, and that this inhomogeneity would make the constancy of rip spacing difficult to judge. To test this, the spacings between consecutive rips were computed versus alongshore location (defined as the mean locations of the consecutive rips). These data were binned into 50 m alongshore location bins and the mean rip spacings for each bin found (Figure 10). By the central limit theorem, confidence limits are based on the standard deviation of rip spacing averaged over the alongshore subdomain from 600 to 1600 m (89.4 m), divided by the square root of the number of degrees of freedom in each bin. Because the rip spacing data are sparse in time and autocorrelated, an average decorrelation time, τ_0, was found from the area under the autocorrelation function for each alongshore bin, and the number of degrees of freedom approximated by the number of temporal bins of width τ_0 (found to be 10.7 days) in which any data occurred. From Figure 10, it is clear that the data are homogeneous (with the exception of a small number of estimates at the beach ends) and the statistical sampling sound.

[25] Initial visual inspection of rip trajectories in Figure 4 suggests a quasi-regular spacing. One of the key objectives

Table 2. Rip System Reset Table, Based on Manual Assessments of Four Experienced Investigators and an Objective Statistic[a]

τ_i	$H^2/\cos(\theta)$	GS	ET	RR	RH
15 Feb 1996	X				X
18 March 1996			X		
30 March 1996		X	X		
4 May 1996	X	X	X	X	X
14 July 1996		X	X	X	X
28 July 1996	X	X	X		
19 Aug 1996		X			
30 Aug 1996	X	X	X	X	
18 Nov 1996		X	X		X
7 Jan 1997		X			
30 Jan 1997		X			
12 Feb 1997	X				
7 April 1997					X
19 April 97					X
1 May 1997			X		
5 May 1997					X
10 May 1997	X	X	X	X	X
15 June 1997	X	X			
29 June 1997	X				
6 Sept 1997			X		
7 Oct 1997	X	X	X		X
12 Dec 1997			X		
9 Jan 1998					X
28 Jan 1998			X		
8 March 1998	X	X		X	X
22 April 1998				X	
5 May 1998	X	X	X	X	
18 May 1998	X				
5 June 1998	X	X	X		
11 June 1998	X				
2 July 1998	X				
16 July 1998	X				
7 Aug 1998	X	X		X	
19 Aug 1998	X				
27 Aug 1998	X				
28 Oct 1998		X		X	X
3 Nov 1998	X				
6 Feb 1999	X	X	X	X	X
7 April 1999	X				
23 April 1999	X	X	X	X	X
2 July 1999	X				
14 July 1999	X	X			X
16 Aug 1999	X				
13 Sept 1999	X				
9 Nov 1999			X		
Total	27	20	18	11	15

[a]Resets shown in the text were based on those with at least three of five votes. Investigators are GS, G. Symonds; ET, E. B. Thornton; RR, R.

of rip current generation models is prediction of this length scale. However, more careful inspection shows that rip spacing often varies considerably in the alongshore direction such that a single spacing is not particularly representative. To quantify this, the standard deviation of rip spacing was computed for each day for which at least four rips had been identified and was normalized by the mean rip spacing for each day to yield a coefficient of variation, plotted as a time series in Figure 11. The mean coefficient of variation was 38.7%, a rather large value. If the spacing were considered to be a Gaussian variable, the 95% confidence interval on rip spacing would be ±1.96*38.7 = 75.8% variation. The calculation was carried out a second time, but after an alongshore trend was removed from the spacing data for each individual day. The mean coefficient of variation remained high, at 33.4%. This large natural variation in characteristic length scale raises questions about its diagnostic value for models that predict only single values of length scale for any set of conditions.

[26] It is possible that rip systems are more rhythmic immediately following system resets, prior to potential reorganization by nonlinear mechanisms. However, visual examination of Figure 11 does not support this hypothesis. The mean value of the coefficient of variation was computed for the first occurrence of rips after each reset. The mean of this set of values was 41% with a standard deviation of 20%. Thus there is no evidence from the data that initial rip formation has better defined rip spacing than at any other time after formation.

[27] Time series of the mean spacing of adjacent rips along with the bar crest position, x_b, a proxy for bulk surf zone width, are shown in Figure 12, with vertical lines indicating times of system reset. The tendency of high-wave events associated with system resets to drive the bar offshore is apparent in most cases and can be confirmed by visual alignment of Hrms time series (Figure 6) and resets in Figure 12. However, the dependence of mean rip spacing on the bar position after these resets is not obvious. To test this characteristic of some rip generation models, the rip spacing after resets were computed as the mean of the spacings for the first 3 days following the first observation of rips after each reset. Bar positions were defined as the mean position between each time of reset and the time of the first following rip spacing observation. Comparing mean rip spacings with bar positions (Figure 13), no statistical dependence is found ($R^2 = 0.0$).

[28] It is still possible that the mean rip spacing, as poorly defined as it may be, scales with bar position throughout the bulk of the time series. In fact, the mean ratio of rip spacing to bar crest position was 4.21, consistent with expectations from instability theories. However, in Figure 12, it appears there are a number of periods when rip spacing systematically decreases over more than 1 month (e.g., August–September 1997, early April 1998, late June to early August 1998, November 1998 to January 1999) where there is no obvious corresponding change in bar crest position. The possibility of a relationship was tested by regressing the running-average rip spacing on the equivalently smoothed bar position. A running average timescale of 10 days was used, but the result was fairly robust to this value. The scatterplot of the smoothed variables, as well as the best linear fit, is shown in Figure 14. While there is considerable scatter, the fit is significant, with values

$$d = (1.51 \pm 0.24)x_b + (105 \pm 15). \quad (3)$$

However, only 16% of the data variance is explained by the relationship. Equation (3) suggests that the bulk ratio for d/x_b of 4.2 is less an indication of a dynamic dependency (best fit slope of 1.5) than a simple statistical average.

4.3. Rip Duration

[29] The previous section discussed the statistics of rip channel location and spacing. The focus of this section is the statistics associated with individual rip trajectories. In all, 389 rip trajectories were identified. The lifetime of any rip channel, T_r, can simply be found as the difference of the

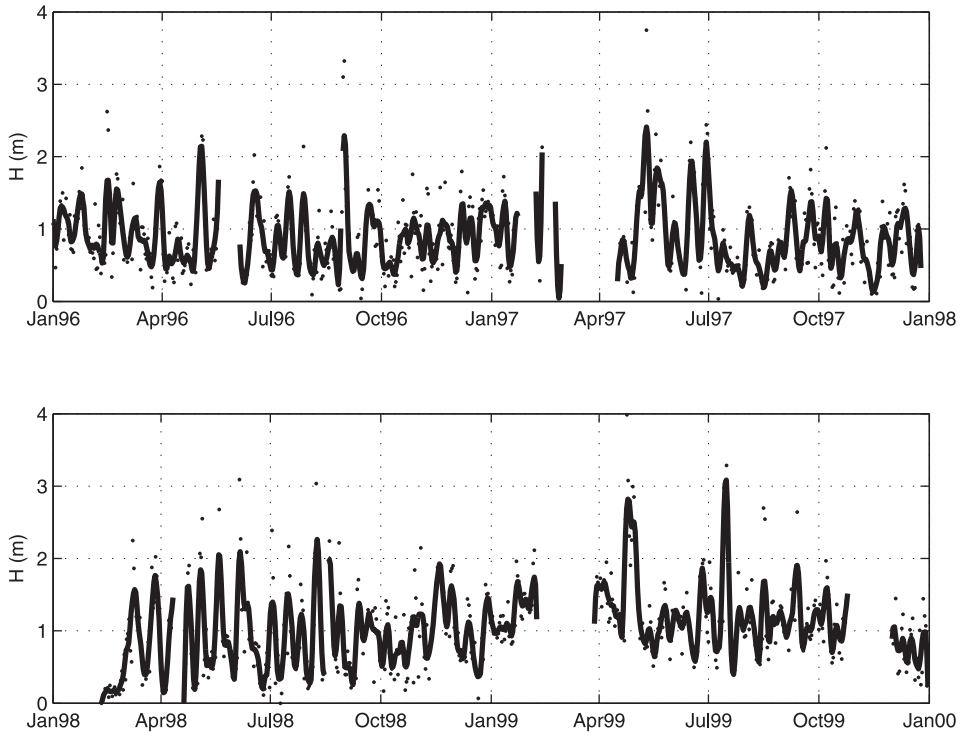

Figure 6. Time series of RMS wave height at 10 m depth. Dots indicate daily mean values while the line is low passed with a 12-day cutoff.

last and first dates of occurrence plus 1 day. Sixty-five rip trajectories were found to have lifetimes of only 1 day. While in some cases this may have been a purely ephemeral feature, in most cases it is likely that these may have been continuing features but were isolated only because no clear connection to an adjoining trajectory could be identified (at times due to data gaps). These cases were neglected, leaving 324 remaining rip current trajectories.

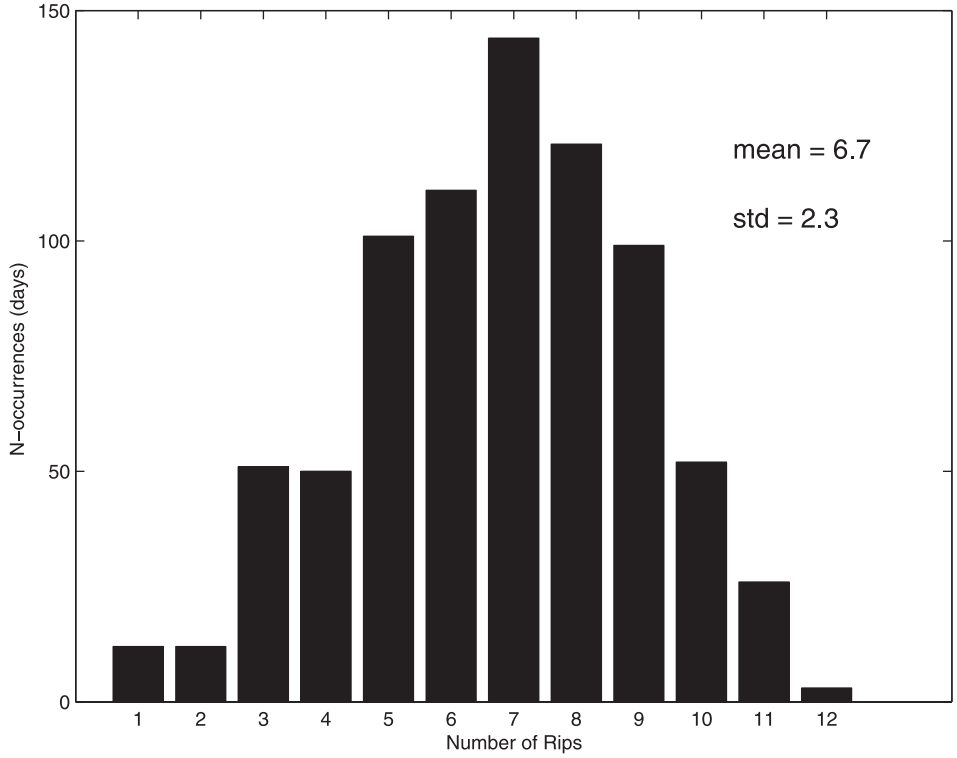

Figure 7. Histogram of the number of rips present at Palm Beach on each day from 1996 to 1999.

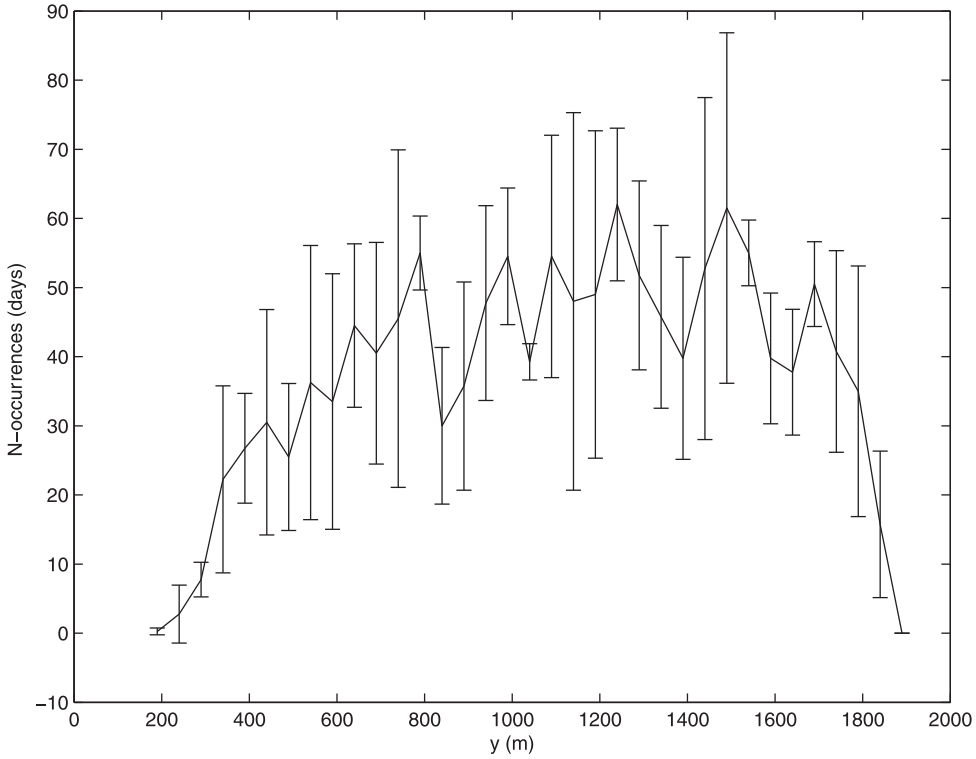

Figure 8. Histogram of rip current occurrences as a function of longshore location. Values and 95% confidence intervals were based on mean and standard deviation of statistics for each of the 4 years of sampling.

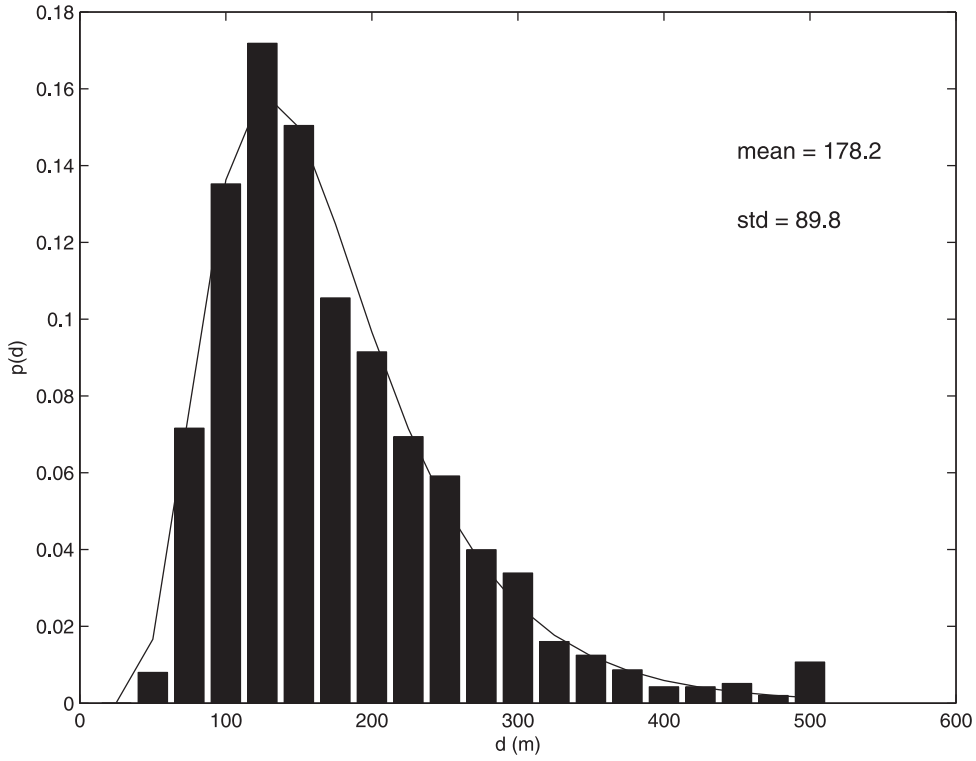

Figure 9. Probability distribution of rip current spacing. The mean and standard deviation are 178.2 and 89.8 m, respectively. The solid curve, a best fit lognormal curve for the same data, shows that the data are well described by this form.

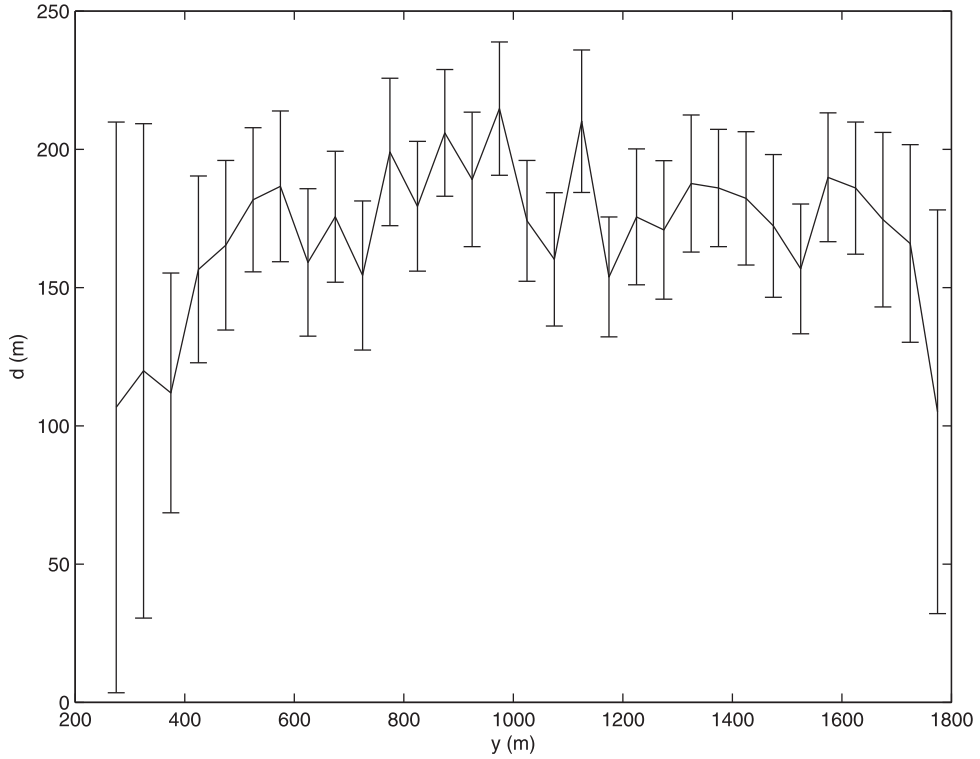

Figure 10. Rip spacing versus mean longshore location based on all rip pair occurrences. The data have been binned by longshore location (50 m bins), and the mean spacing has been plotted to detect the possible presence of a longshore trend. No such trend was found. Error bars correspond to 95% confidence limits.

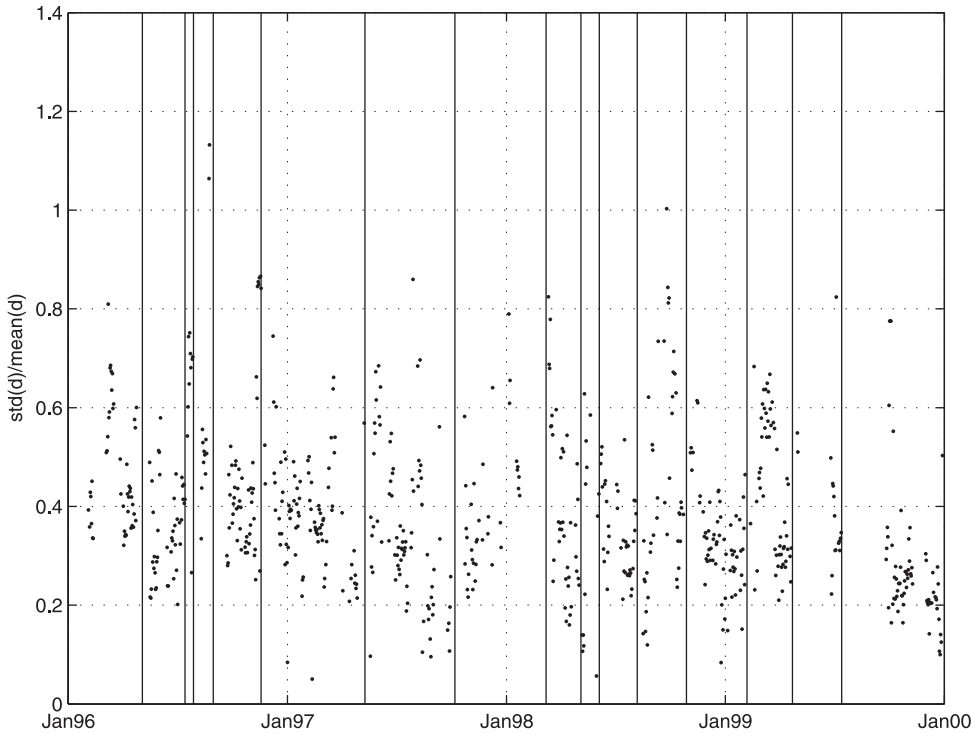

Figure 11. Fractional variation in rip spacing, defined by the standard deviation divided by the mean, for each day of sampling. System resets are indicated by vertical lines.

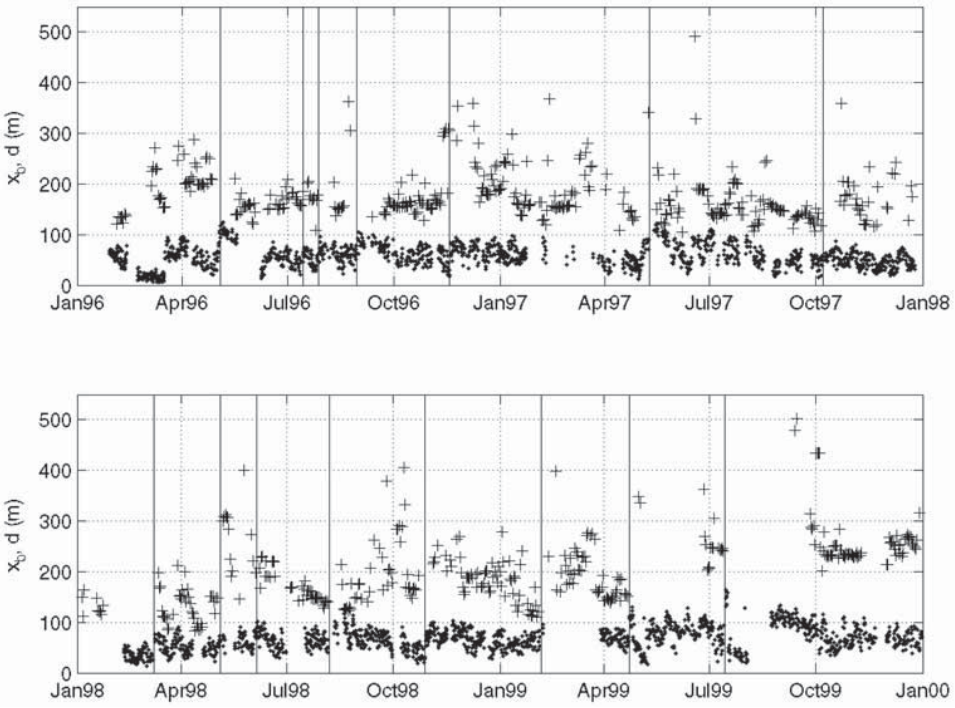

Figure 12. Time series of bar crest position (dots) and alongshore mean rip spacing (pluses). Times of system reset are shown by vertical lines. Wave height (Figure 6) is plotted to the same scale to allow direct comparison.

[30] From Figure 4, it was apparent that the lifetime of rip currents, while variable, can be quite long. To quantify this, a histogram of rip lifetime was computed (Figure 15). To avoid biasing the statistics by the larger number of short-duration rip trajectories, the histogram statistics were weighted (multiplied) by the lifetime for each bin. The resulting probability distribution indicates the probability of rip channels that are present on any day having a particular lifetime. Observed rip lifetimes are significantly variable with a mean lifetime of 45.6 days (computed from the first moment of the distribution function).

[31] The above statistic represents the expected lifetime of any single rip current within a longer-lived field of rip currents. From Figure 4, it is clear that fields of rip channels are generally present, except for short periods of time after system resets (excluding data gaps when the condition of rip channels is unknown). The mean formation time between reset events and the first, clear identification of subsequent rip currents was 7.7 days (excluding the 61-day period of low waves and confusing morphology starting in July 1999). Thus these alongshore uniform initial conditions represent only 8.4% of the sampling period.

4.4. Rip Mobility

[32] From the trajectory data, $\mathbf{y_i}(t)$, rip migration rates were computed as the difference in daily rip locations. For the entire set of data, the RMS migration rates were found to be 17.1 m/day, implying a rather mobile system. However, part of the mobility signal results from a digitization noise error of ±12 m, discussed previously. Undertaking the same calculation on an ensemble of times sequences of synthetic Gaussian white noise with RMS values of 12 m yielded an RMS migration rate of 17.6 m/day, implying that the observed value based on daily migration rate statistics was indistinguishable from noise. However, for migration rates computed over longer spans, the effect of noise is reduced. For data based on net migration over an 8-day span, the observed RMS migration rate was 4.5 m/day, double the 2.2 m/day rate from the synthetic noise test. A histogram of 8-day migration rates (Figure 16), shows that rates greater than 5 m/day are common with a maximum value of 20 m/day averaged over one 8-day span. Of the 5329 migration rate estimates, 2981 (56%) exceeded the 2.2 m/day rate from synthetic noise tests. It is also evident from Figure 16 that rip channel migration is equally likely to occur in either direction (southward or northward) along the beach.

[33] Visual inspection of rip trajectories in Figure 4 suggest that there may be periods when the entire rip system migrates relatively uniformly, presumably in response to wave forcing. To test whether a bulk migration rate varies with bulk forcing, it was first necessary to determine if a bulk migration rate is, in fact, a useful statistic. For each day for which migration rates were available from at least four different rips, the mean and standard deviation rates were computed, $\langle V \rangle$ and σ_V, respectively. A coefficient of variation was then computed as $\sigma_V(t_i)/|\langle V \rangle|$. While this number can be large since $\langle V \rangle$ can approach zero, none of the values were small enough to consider the alongshore average migration rate to be a representative number. Even for the 87 (out of 727) cases when the magnitude of $\langle V \rangle$ was greater than 5 m/day, the

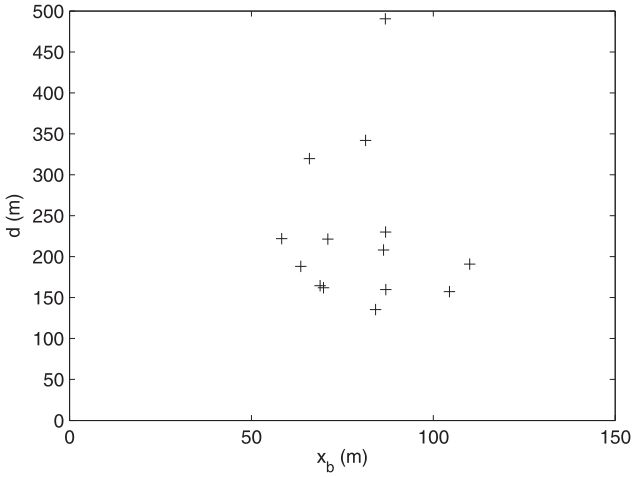

Figure 13. Dependence of mean rip spacing on bar crest location at times of rip formation. Rip spacing data are averaged over the first 3 days after rip generation. Bar location is the average between the time of system reset and the first observation of bar generation. The R^2 of the relation is 0.0.

mean coefficient of variation was 66% (implying a large 95% confidence limit of 129% variation, if Gaussian statistics were assumed).

[34] Nevertheless, the mean migration rate was compared to a proxy for the mean alongshore current ($v_L = (gH_s)^{1/2}$ sin(θ) cos(θ) [*Komar*, 1998], but using offshore wave height instead of a break point value). The scatter was very large but the relationship was significant with an R^2 of 0.78, a best fit slope of 5.4, and an RMS error of 2.87 m/day (Figure 17). *Ruessink et al.* [2000] also found a dependence of crescentic bar migration rates on a similar quantity, the longshore component of wave energy flux.

5. Discussion

[35] Theories for rip current generation have typically been based on studies from simplified laboratory situations or numerical models forced by monochromatic waves and generally seek to explain the dominant alongshore rip spacing at the time of formation, assumed to be the most diagnostic observable. Subsequent evolution of the system, after the development of topographic channels, requires modeling of the full, coupled fluid-morphology system in a stochastic setting and is not associated with simple expectations.

[36] Many of the existing models do not appear to have any predictive capability. The models of *Bowen* [1969] and *Bowen and Inman* [1969], based on synchronous edge waves, predicts scales that are an order or magnitude below the mean spacing of 178 m [*Ranasinghe et al.*, 1999]. The observed rips showed no preferred location, and hence are inconsistent with models due to edge waves trapped in a pocket beach. The *Dalrymple* [1975] model can produce longer rip spacing, but requires an unrealistic, phase-locked bidirectional wave field. Instability models commonly suggest that rip spacing should be about four times the surf zone width (or bar crest position, as the two variables

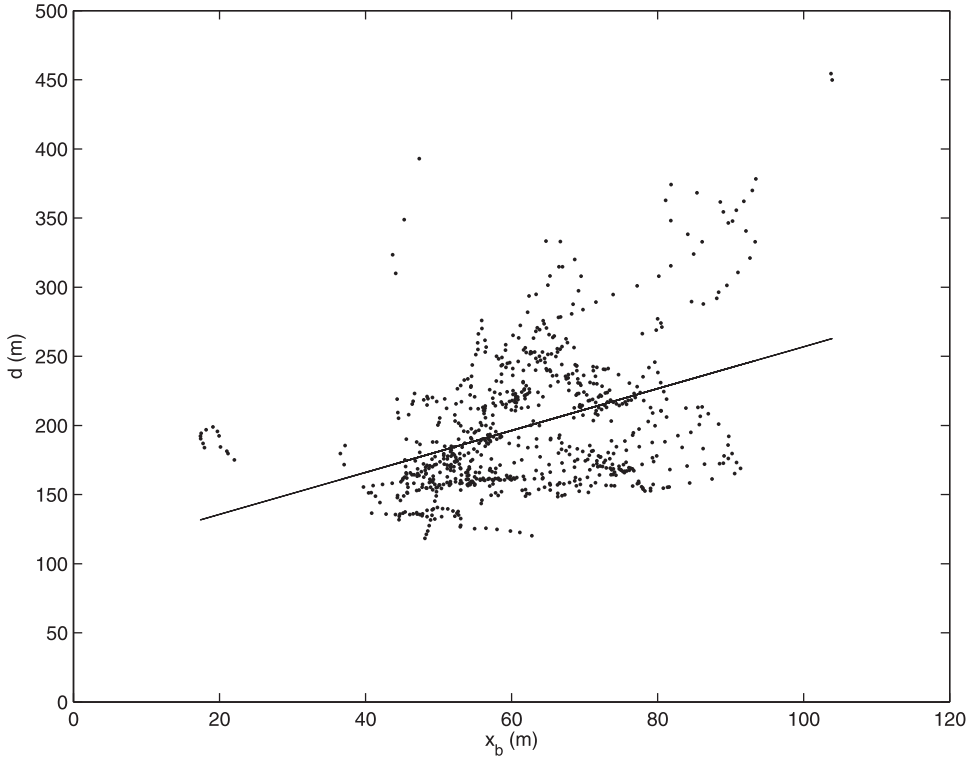

Figure 14. Dependence of running average mean rip spacing versus bar crest position for the full 4 years of data. Line indicates best fit, $d = (1.51 \pm 0.24)x_b + (105 \pm 15)$. Running average time constant was 10 days.

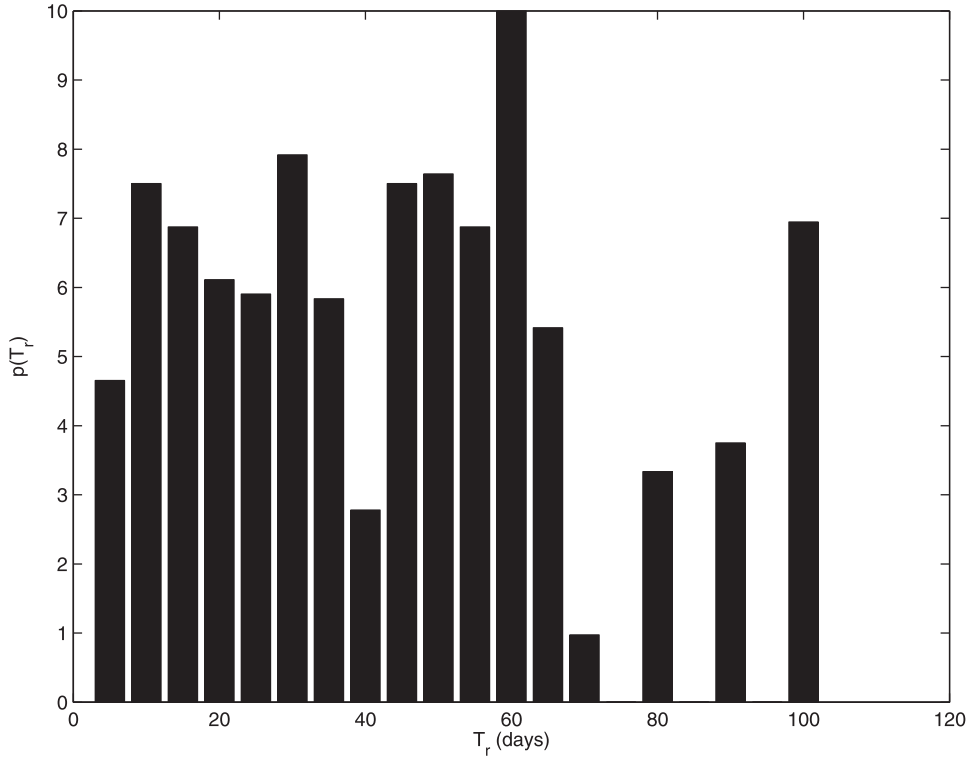

Figure 15. Probability distribution of rip current lifetimes, T_r, expressed as a percentage. Histogram counts for each bin have been weighted by rip lifetime for that bin so that the histogram represents the probability that a rip, observed on any particular day, will have a particular lifetime.

commonly scale). However, tests for cases of initial rip formation after a system reset show no significant relationship and, while the bulk ratio of rip spacing to bar crest position is 4.2, the slope of the best fit regression is only 1.5.

[37] Several further problems exist with application of these rip generation models to natural environments. First, the data presented in this paper show that the alongshore uniform initial conditions assumed by most rip generation models are rare, spanning only 8.4% of the data record. Thus models that assume alongshore uniform initial conditions have, at most, very limited applicability. Second, these data show that while the primary observable statistic, rip spacing, appears quasiperiodic, it is instead highly variable with a coefficient of variation of around 39% (a 95% confidence limit of 76%). Only the models incorporating stochastic variability by *Damgaard et al.* [2002] (seabed perturbations) and *Reniers et al.* [2004] (directional wave spectrum) properly simulate variations in rip spacing. Interestingly, *Reniers et al.* [2004] predict a coefficient of variation of 36% over the nominal range of mean directional spread of 5°–22°, in agreement with the measurements presented here.

[38] Estimates of rip migration rates are hindered by the ±12 m RMS error associated with manual rip location identification. Movie loop visualization of rectified images shows a remarkably mobile system and the RMS migration rate for the entire data set is 17 m/day, with considerable short-term variability in both direction and rate. However, the ''true'' short-term variability cannot be statistically separated from noise, so a conservative approach has been taken of neglecting these short-term signals to characterize only longer-term rates. The fact that 8-day mean migration rates were significantly greater than measurement error in 56% of cases does not imply that shorter-term variations were insignificant (just unresolvable). Eight-day migration rates showed a significant correlation with similarly smoothed wave forcing, with 78% of the variance explained by a linear relationship.

[39] Several alternate approaches exist in the literature for estimation of longshore migration rates of sandbar morphologies. *Ruessink et al.* [2000] used a complex EOF technique to characterize variability of bar crest position over a 500 m longshore extend of the Dutch coast. From time and longshore phase information of the first EOF, migration rates of up to 150 m/day were found. Similarly, longshore lag correlation analysis between consecutive bar crest maps can yield objective measures of longshore migration. However, both these techniques are based on a variable, bar crest position, that is a continuous function of longshore location and are not possible for the rip trajectory type of data used in this paper.

[40] There is considerable overlap between studies of longshore variability of sandbar systems and of rip currents that are commonly located at the embayments of crescentic bars. For bar systems with ratios of cross-shore to longshore length scale approaching 1.0, circulation and rips are driven by superelevation of sea level over the horns of the bar system and the two components (rip channels and crescentic bars) are intimately tied. However, as the ratio of cross-shore to longshore scales becomes much less than 1.0, pressure gradients become smaller and the generation of a

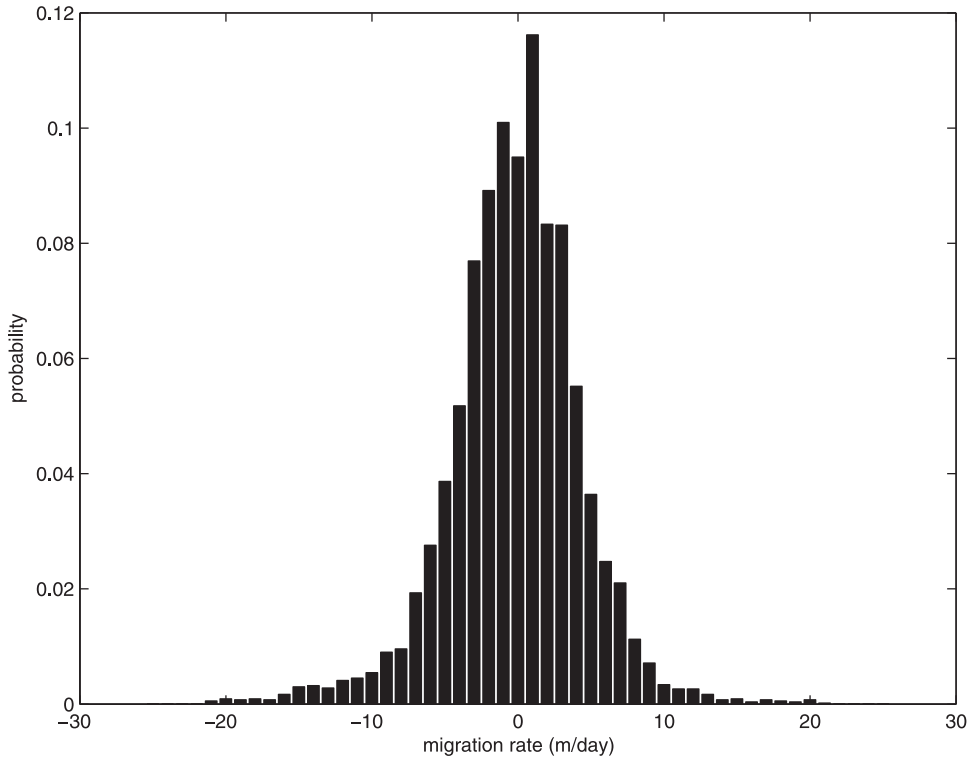

Figure 16. Histogram of rip migration rates, computed as the mean rate over 8-day windows, stepping through all of the rip trajectories that exceeded a 9-day length.

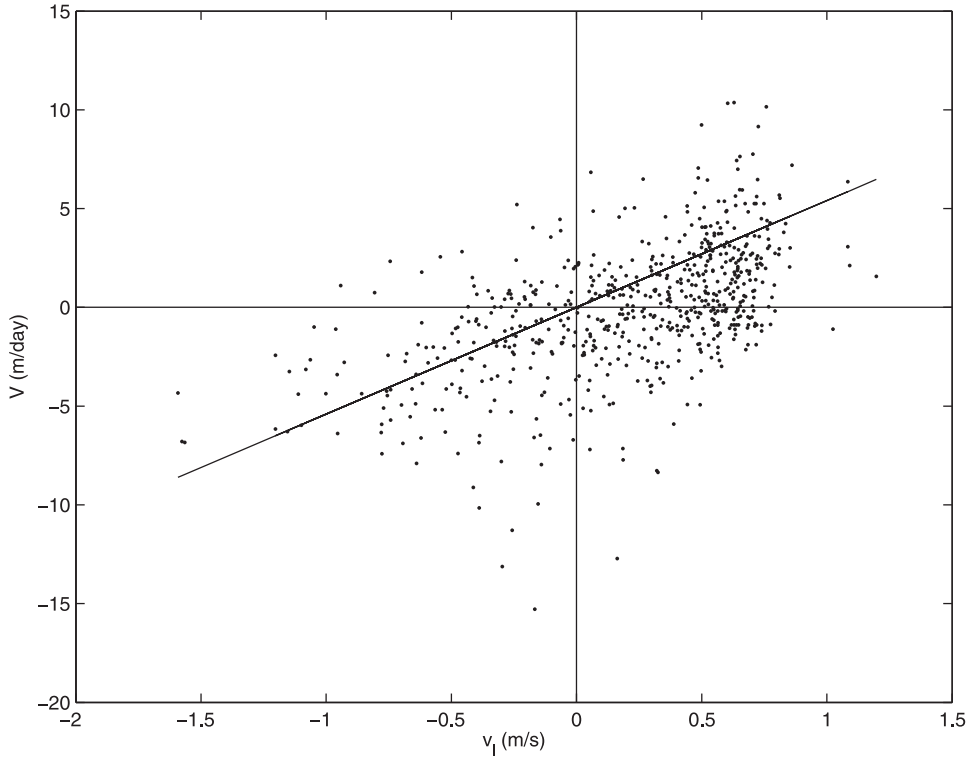

Figure 17. Observed 8-day mean rip migration rates, V, versus a proxy for longshore current, v_l, similarly smoothed to an 8-day running mean. Line indicates the least squares fit with slope 5.4.

narrow offshore jet (a rip) becomes less likely. Comparison of the rip migration rates discussed in this paper with the observations by *Ruessink et al.* [2000] of migration rates of 150 m/day, reversing on an almost daily basis, should not be interpreted as meaning that the rip currents at Palm Beach are stagnant. The Dutch data come from a system with a low cross-shore to longshore length scale that can yield large changes in longshore phase due to small perturbations in bar crest position.

6. Conclusions

[41] A 4-year data set of daily time exposure images has been analyzed to describe the statistics of a natural rip current system at Palm Beach, Australia, an embayed beach located in a microtidal, swell-dominated coastal environment. A total of 5271 rips were observed over 782 days, an average of 6.7 rips per day (data were not available or rips were not present on 646 days). The probability of rip occurrence was uniform along this beach, with no indication of preferred alongshore locations that might be associated with standing edge waves trapped between headlands. The 324 individual rip channel trajectories were long-lived, lasting 45.6 days on average. Moreover, the complete destruction of the rip system, such that the initial conditions for subsequent rip generation were alongshore uniform, was rare, occurring only every 91 days on average (four times per year) and comprising only 8.4% of the record.

[42] The mean rip spacing for the 4 years was 178 m and the distribution was well modeled as a lognormal distribution. However, rip spacing typically showed strong alongshore variability with a mean coefficient of variation (standard deviation/mean) of 39%. Thus, if the statistics were assumed Gaussian, the 95% variation in rip spacing would be ±76%. Rip spacing showed no systematic alongshore dependence. The average ratio of mean rip spacing to bar crest distance from the shoreline, x_b, was 4.21, consistent with some instability models, and the correlation of the two variables was slightly significant but explained only 16% of the variance and the slope of the regression was 1.5, not 4. In contrast, the mean rip spacing after reset events (when the initial conditions for models are met) showed a larger coefficient of variation (41%) than for the bulk data and showed no significant correlation with x_b. Thus models for rip formation that are based on the alongshore uniform assumption or that predict a single rip spacing appear not to be generally applicable to this type of beach. Models incorporating stochastic variability such as *Reniers et al.* [2004] predict mean and variability of alongshore spacing of rip currents consistent with these measurements.

[43] Rips tended to be mobile, with the mean absolute 8-day average velocity of 2.4 m/day. 56% of the velocity estimates exceeded 2.2 m/day, the 95% confidence limit on noise. As with rip spacing, the mean migration rate of the system showed strong longshore variability and was typically not well defined. Even for mean migration rates greater than 5 m/day, the mean coefficient of variation was 66% (95% confidence interval of 129%). A linear relationship between the mean migration rate (poorly defined) and a proxy for the longshore current explained 78% of the variance with an RMS error of 2.87 m/day and a slope of 5.4 m/day per m/s.

[44] **Acknowledgments.** The wave and tide gauge data were kindly provided by the Manly Hydraulics Laboratory, Sydney. This work was funded by the U.S. Office of Naval Research under Coastal Geosciences, grants N00014-02-1-0154 and N00014-04-WR20066; the International Cooperative Opportunities in Science and Technology Program (NICOP), grant N00014-97-1-0789; and the National Science Foundation, grant OCE-0136882. R.H. would like to thank the Andrew Mellon Foundation and the U.S. Geological Survey for making development of the Argus Program possible. Much work on this manuscript was done while G.S. was on a research associateship award from the National Research Council of the National Academies at the Naval Postgraduate School in Monterey, California. Ad Reniers assisted with the HISWA predictions, and Soupy Alexander kindly provided time series of bar location. Their assistance is gratefully acknowledged. We thank Nalin Wikramasinghe for help in image rectification and analysis. The comments of anonymous reviewers were very helpful in improving this manuscript.

References

Aarninkhof, S., and R. A. Holman (1999), Monitoring the nearshore with video, *Backscatter*, *10*(2), 8–11.

Alexander, P. S., and R. A. Holman (2004), Quantitative analysis of nearshore morphological variability based on video imaging, *Mar. Geol.*, *208*, 101–111.

Blondeaux, P. (2001), Mechanics of coastal forms, *Annu. Rev. Fluid Mech.*, *33*, 339–370.

Bowen, A. J. (1969), Rip currents: 1. Theoretical investigations, *J. Geophys. Res.*, *74*(23), 5467–5478.

Bowen, A. J., and D. L. Inman (1969), Rip currents: 2. Laboratory and field observations, *J. Geophys. Res.*, *74*(23), 5479–5490.

Bowen, A. J., and D. L. Inman (1971), Edge waves and crescentic bars, *J. Geophys. Res.*, *76*(36), 8662–8671.

Brander, R. W. (1999), Field observations on the morphodynamic evolution of a low-energy rip current system, *Mar. Geol.*, *157*, 199–217.

Dalrymple, R. A. (1975), A mechanism for rip current generation on an open coast, *J. Geophys. Res.*, *80*, 3485–3487.

Dalrymple, R. A., and C. J. Lozano (1978), Wave-current interaction models for rip currents, *J. Geophys. Res.*, *83*, 6063–6071.

Damgaard, J., N. Dodd, J. Hall, and T. Chesher (2002), Morphodynamic modeling of rip channel growth, *Coastal Eng.*, *45*, 199–221.

Deigaard, R., N. Drønen, J. Fredsøe, J. Jensen, and M. A. Jorgensen (1999), Morphological stability analysis for a long straight barred coast, *Coastal Eng.*, *36*, 171–195.

Falques, A., A. Montoto, and D. Vila (1999), A note on hydrodynamic instabilities and horizontal circulation in the surf zone, *J. Geophys. Res.*, *104*(C9), 20,605–20,615.

Falques, A., G. Coco, and D. A. Huntley (2000), A mechanism for the generation of wave-driven rhythmic patterns in the surf zone, *J. Geophys. Res.*, *105*(C10), 24,017–24,087.

Hino, M. (1974), Theory of the formation of rip-current and cuspoidal coast, paper presented at 14th International Conference on Coastal Engineering, Am. Soc. of Civ. Eng., Copenhagen.

Holland, K. T., R. A. Holman, T. C. Lippmann, J. Stanley, and N. Plant (1997), Practical use of video imagery in nearshore oceanographic field studies, *IEEE J. Oceanic Eng.*, *22*(1), 81–92.

Holman, R. A. (1995), Nearshore processes, *U.S. Natl. Rep. Int. Union Geod. Geophys. 1991–1994*, *Rev. Geophys.*, *33*, 1237–1247.

Holman, R. A., J. A. H. Sallenger, T. C. Lippmann, and J. W. Haines (1993), The application of video image processing to the study of nearshore processes, *Oceanography*, *6*(3), 78–85.

Holman, R. A., J. Stanley, and T. H. Özkan-Haller (2003), Applying video sensor networks to nearshore environmental monitoring, *IEEE Pervasive Comput.*, *2*(4), 14–21.

Holthuijsen, L. H., N. Booij, and T. H. C. Herbers (1989), A prediction model for stationary, short-crested waves in shallow water with ambient currents, *Coastal Eng.*, *17*, 211–225.

Huntley, D. A., and A. D. Short (1992), On the spacing between observed rip currents, *Coastal Eng.*, *17*, 211–225.

Komar, P. D. (1998), *Beach Processes and Sedimentation*, 554 pp., Prentice-Hall, Upper Saddle River, N. J.

Lippmann, T. C., and R. A. Holman (1989), Quantification of sand bar morphology: A video technique based on wave dissipation, *J. Geophys. Res.*, *94*(C1), 995–1011.

Murray, A. B., and G. Reydellet (2001), A rip-current model based on a newly hypothesized interaction between waves and currents, *J. Coastal Res.*, *17*, 517–531.

Ranasinghe, R., G. Symonds, and R. A. Holman (1999), Quantitative characterization of rip currents via video imaging, in *Coastal Sediments '99*, edited by N. C. Kraus and W. G. McDougal, pp. 987–1002, Am. Soc. of Civ. Eng., Reston, Va.

Ranasinghe, R., G. Symonds, K. Black, and R. A. Holman (2004), Morphodynamics of intermediate beaches: A video imaging and numerical modeling study, *Coastal Eng.*, *51*, 629–655.

Reniers, A., G. Symonds, and E. B. Thornton (2001), Modeling of rip currents during RDEX, in *Coastal Dynamics '01*, edited by H. Hanson and M. Larson, pp. 493–499, Am. Soc. of Civ. Eng., Reston, Va.

Reniers, A. J. H. M., J. A. Roelvink, and E. B. Thornton (2004), Morphodynamic modeling of an embayed beach under wave group forcing, *J. Geophys. Res.*, *109*, C01030, doi:10.1029/2002JC001586.

Ruessink, B. G., I. M. J. van Enckevort, K. S. Kingston, and M. A. Davidson (2000), Analysis of observed two- and three-dimensional nearshore bar behaviour, *Mar. Geol.*, *169*, 161–183.

Shepard, F. P., K. O. Emery, and E. C. La Fond (1941), Rip currents: A process of geological importance, *J. Geol.*, *49*, 337–369.

Short, A. D. (1985), Rip current type, spacing and persistence, Narrabeen Beach, Australia, *Mar. Geol.*, *65*, 47–71.

Short, A. D., and N. L. Trenaman (1992), Wave climate of the Sydney region, and energetic and highly variable ocean wave regime, *Aust. J. Mar. Freshwater Res.*, *43*, 765–791.

Symonds, G., R. A. Holman, and B. Bruno (1997), Rip currents, in *Coastal Dynamics '97*, edited by E. B. Thornton, pp. 584–593, Am. Soc. of Civ. Eng., Reston, Va.

van Enckevort, I. M. J., and B. G. Ruessink (2001), Effect of hydrodynamics and bathymetry of video estimates of nearshore sand bar position, *J. Geophys. Res.*, *106*(C8), 16,969–16,979.

van Enckevort, I. M. J., B. G. Ruessink, G. Coco, K. Suzuki, I. L. Turner, N. G. Plant, and R. A. Holman (2004), Observations of nearshore crescentic sandbars, *J. Geophys. Res.*, *109*, C06028, doi:10.1029/2003JC002214.

Werner, B. T. (1999), Complexity in natural landform patterns, *Science*, *284*, 102–104.

Wright, L. D., and A. D. Short (1984), Morphodynamic variability of surf zones and beaches: A synthesis, *Mar. Geol.*, *56*, 93–118.

Wright, L. D., F. C. Coffey, and P. J. Cowell (1980), Nearshore oceanography and morphodynamics of the broken bay—Palm Beach region, N. S. W.: Implications for offshore dredging, Coastal Stud. Unit, Dep. of Geogr., Univ. of Sydney, Sydney, N. S. W., Australia.

R. A. Holman, College of Oceanic and Atmospheric Sciences, Oregon State University, Corvallis, OR 97331-5503, USA. (holman@oce.orst.edu)

R. Ranasinghe, Department of Infrastructure, Planning and Natural Resources, University of New South Wales, Sydney, NSW 2124, Australia.

G. Symonds, Floreat Marine Laboratories, CSIRO, Underwood Avenue, Floreat Park, WA 6014, Australia.

E. B. Thornton, Oceanography Department, Naval Postgraduate School, Monterey, CA 93943, USA.